

Flow behavior of high internal phase emulsions and preparation to microcellular foam

Seong Jae Lee*

Department of Polymer Engineering, The University of Suwon,
San 2-2, Wau-ri, Bongdam-eup, Hwaseong, Gyeonggi 445-743, Korea
(Received July 19, 2004; final revision received September 11, 2004)

Abstract

Open microcellular foams having small-sized cell and good mechanical properties are desirable for many practical applications. As an effort to reduce the cell size, the microcellular foams combining viscosity improvers into the conventional formulation of styrene and water system were prepared via high internal phase emulsion polymerization. Since the material properties of foam are closely related to the solution properties of emulsion state before polymerization, the flow behavior of emulsions was investigated using a controlled stress rheometer. The yield stress and the storage modulus increased as viscosity improver concentration and agitation speed increased, due to the reduced cell size reflecting both a competition between the continuous phase viscosity and the viscosity ratio and an increase of shear force. Appreciable tendency was found between the rheological data of emulsions and the cell sizes of polymerized foams. Cell size reduction with the concentration of viscosity improver could be explained by the relation between capillary number and viscosity ratio. A correlative study for the cell size reduction with agitation speed was also attempted and the result was in a good accordance with the hydrodynamic theory.

Keywords : high internal phase emulsion, microcellular foam, rheological properties, cell size

1. Introduction

High internal phase emulsions (HIPEs) or high internal phase ratio emulsions (HIPREs) are classified as emulsions with an internal phase volume above 74.05% for mono-disperse spheres. Such systems are biphase foams with the continuous phase forming lamella between the distorted droplets of the internal phase. They have a number of actual and potential applications, some of which are mayonnaise in food, gels and creams in cosmetic products, petroleum gels as safety fuels, oil recovery from oil sands, and agricultural sprays with pesticidal properties (Cameron and Sherrington, 1996; Park *et al.*, 2003). One of the most important applications of HIPEs is their ability to be used as open foams by the polymerization of oil phase (Barby and Haq, 1982). Open microcellular foams with low density prepared by the high internal phase emulsion polymerizations, known as polyHIPE, show highly porous characteristics with regular, spherical and isotropic structure. The cellular structure of polyHIPE is quite different from the oriented, irregular and anisotropic structure of commercial blown and extruded foams that generally contain closed cell morphology with cell sizes of the order of

100 μm . The HIPE foams are currently of interest because of their low density, microstructural and open cell, and high absorbency capabilities. A number of applications include polymeric membranes, ion exchange resin, controlled release systems, absorbents and inertial confinement fusion targets (Bhumgara, 1995; Stokes and Evans, 1997; Duke *et al.*, 1998; Wakeman *et al.*, 1998). The success in these applications strongly depends on the microcellular structure having large surface area, i.e., small cell size. The sizes of both cell and open window between adjacent cells can be controlled by changing the controlling factors, such as mixing method, agitation speed, surfactant concentration and the composition of oil phase during the emulsion preparation. One of the simplest methods to get smaller cell size is to impose higher agitation speed during the preparation of emulsion mixture. Another way to attempt is to increase the viscosity of continuous phase, which might affect the cell size depending on the viscosity ratio of dispersed to continuous phases. To achieve this goal, an incorporation of viscosity improver to the continuous phase is likely to be a good candidate.

In this study, the open microcellular foams combining a high molecular weight polymer, either polybutadiene or polystyrene, into the conventional formulation of styrene and water system were prepared via highly concentrated water-in-oil emulsion (Fig. 1) followed by polymerization.

*Corresponding author: sjlee@suwon.ac.kr
© 2004 by The Korean Society of Rheology

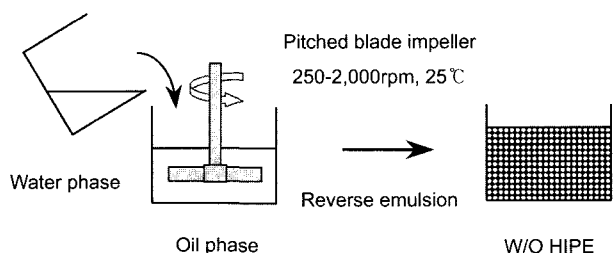


Fig. 1. Schematic diagram for the preparation of water-in-oil HIPE system.

To characterize the emulsions that result in the microcellular foams, the rheological properties of the emulsions were investigated because the resultant foam properties are dependent on the flow behavior of emulsion state before the polymerization of emulsion into foam begins. Steady shear, creep recovery, and oscillatory shear tests were carried out on a series of HIPEs. While a number of literatures have been published on the rheology of dilute and semi-concentrated emulsions, only a little attention has been given to HIPE (Princen, 1983; Princen and Kiss, 1989; Pal, 1999). As a result of this study, there was a match, qualitatively at least, between the rheological data of the emulsions and the cell size change of the polymerized foams. Cell size decrease of the foams with the increase in viscosity improver concentration and agitation speed could be explained as well by the capillary number relation and hydrodynamic analysis describing drop breakup.

2. Experimental

2.1. Materials

The monomers used were styrene (Showa Chemical) and divinylbenzene (DVB; Aldrich). Polybutadiene (PB; Aldrich) and polystyrene (PS; LG Chemical) as viscosity improvers, sorbitan monooleate (SMO) as an emulsifier and potassium persulfate (KPS) as an initiator were also used. Other candidates for viscosity enhancement, such as organoclays, were attempted to prepare the polyHIPE foams with reduced cell size, but the foams incorporated with them were poor in mechanical property sense. Styrene was purified by a vacuum distillation and DVB was washed with 10% NaOH solution followed by water before use. PB has monomer units of 36% cis, 55% trans and 9% vinyl and weight-average molecular weight (Mw) of 420,000 g/mol. PS has Mw of 246,000 g/mol and its polydispersity index is 2.14. SMO has the hydrophile-lipophile balance of 4.3 whose value is known suitable for the formation of water-in-oil emulsions. Distilled water was used throughout the experiments.

2.2. Preparation

Mixture of 11.2 g comprised of styrene and viscosity improver was used as styrene solution. Other components

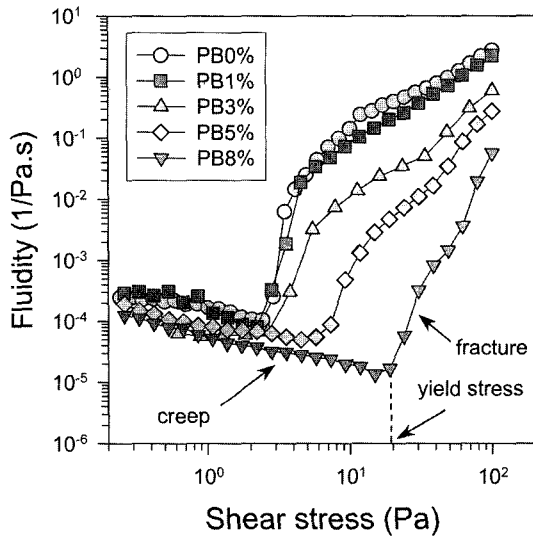
were fixed: 150 g of water, 3.8 g of DVB, 3.43 g of SMO and 0.2 g of KPS. Code numbers, PB x S y and PS x S y were used to identify the PB-series and the PS-series, where x stands for viscosity improver concentration in styrene solution and y stands for the agitation speed. For example, PB3S500 indicates the sample prepared by 3 wt% of PB and 500 rpm of agitation speed. The oil phase consists of monomers, viscosity improver and surfactant. The aqueous phase consists of distilled water and initiator. The oil phase was charged into a beaker and mechanically stirred at a given speed. While the oil phase was stirred, the aqueous phase was added dropwise. Total addition time was 30 min. Emulsion mixture was sealed with parafilm to minimize water evaporation and polymerized for 48 h in a convection oven at 60°C. The polymerized mass was dried to remove water and residual volatiles for several days. Detail description of the emulsion and foam preparation can be found elsewhere (Williams and Wroblewski, 1988; Jeoung *et al.*, 2002; Choi *et al.*, 2003).

2.3. Characterization

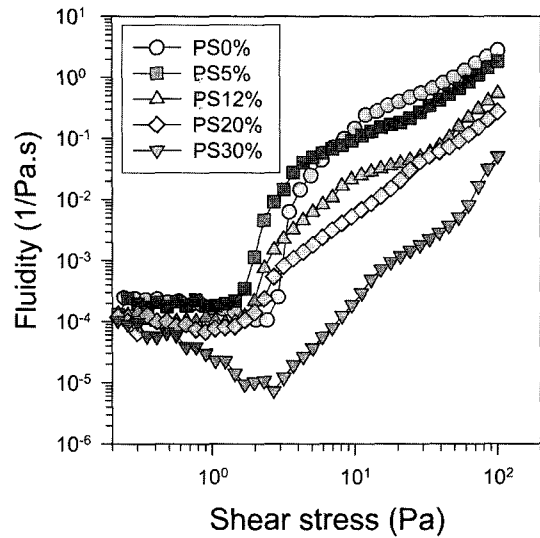
Rheological properties of the emulsions prepared were measured at 25°C in a controlled stress rheometer (MCR 300, Physica) to investigate the emulsion stability, the yield stress and the storage modulus depending on viscosity improver concentration and agitation speed. The foam morphology and cell size were characterized with a scanning electron microscope (SEM 5200, Jeol) from fractured samples. The cell size and size distribution of each sample could be obtained from the image analysis technique that statistically evaluates a number of cell sizes of SEM micrographs.

3. Results and discussion

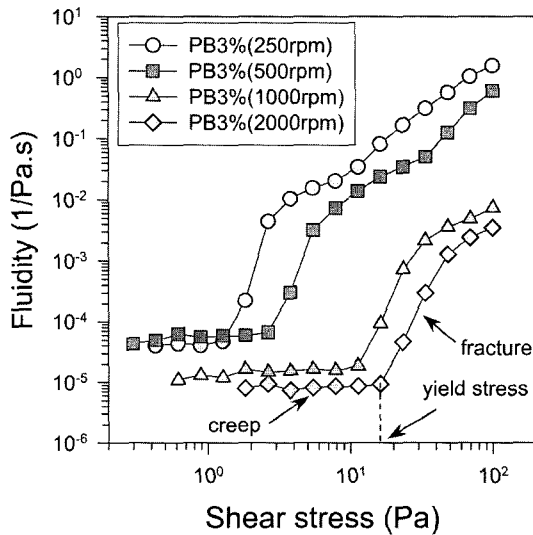
Since the foam morphology and microstructure are dependent on the emulsion properties, measuring the rheological properties of emulsion informs us the regularity and cell size of resultant foam. When HIPEs are subjected to a shear stress below the yield stress, they exhibit very small deformation indicating creep behavior. Fig. 2 shows the fluidity change of PB series as a function of shear stress in a steady shear mode. The fluidity data were obtained from the slope of the shear rate versus shear stress behavior of HIPEs. Thus, the fluidity is the same as the reciprocal of viscosity and means the physical properties of a substance that enables it to flow. The yield stress was determined from the onset point of abrupt increase of fluidity. Upon increasing the shear stress above the yield stress, a large increase in fluidity is observed indicating flowing or fracturing of the material. The yield stress increased with the increase of PB concentration and agitation speed. Fig. 3 shows the corresponding flow behavior for PS series but the yield stress is less dependent on concentration and agi-



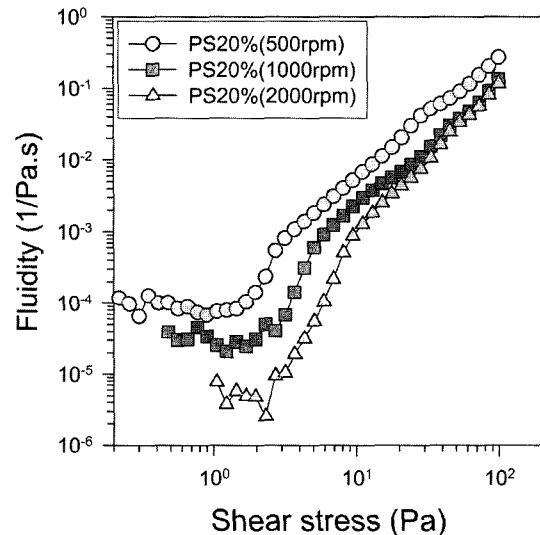
(a)



(a)



(b)



(b)

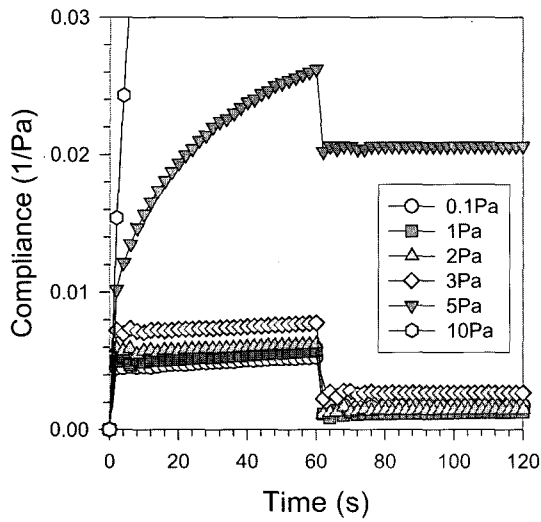
Fig. 2. Fluidity vs. shear stress behavior of HIEs in a steady shear mode: (a) effect of PB concentration and (b) effect of agitation speed.

Fig. 3. Fluidity vs. shear stress behavior of HIEs in a steady shear mode: (a) effect of PS concentration and (b) effect of agitation speed.

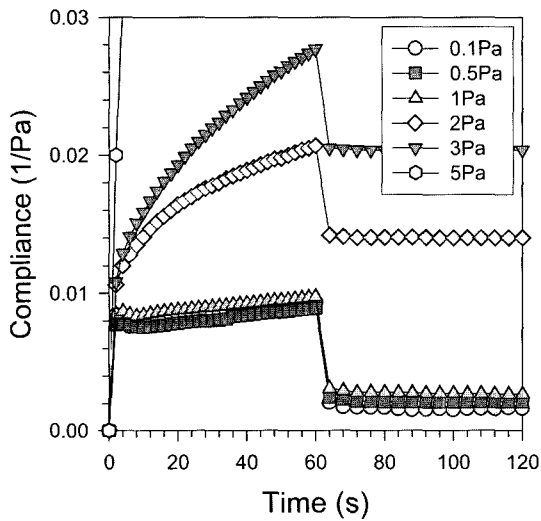
tation speed compared with PB series. The reason for higher yield stress in PB series is speculated from the fact that the characteristic molecular weights of PB, such as critical molar mass and entanglement molar mass, are one order of magnitude smaller than those of PS (Graessley, 1984). Thus the PB having higher molecular weights and even longer chains can have a possibility to generate more entangled structure, resulting in tougher and more elastic emulsion than the PS counterpart.

Using creep curves the linear viscoelastic (LVE) region of a materials response can be easily demonstrated, simply by plotting the compliance responses at several different stresses on the same scale. Since strain is proportional to

stress within the LVE region, the responses will overlap one another on the compliance scale. Upon reaching the yield stress, the compliance curve does not overlap any more and enters the nonlinear region. Fig. 4 shows the creep recovery response of two representative samples: one is for PB3S500 and the other is for PS20S500. The shear compliance is plotted as a function of time at different stress levels. For PB3S500 sample, the emulsion exhibits almost same compliance values within the stress of 2 Pa and nearly same recovery values when the stresses are removed. At the stress of 3 Pa, the emulsion is just at that very moment of start to flow and fracture begins at higher stresses. Thus, the yield stress of this emulsion is about 3



(a)

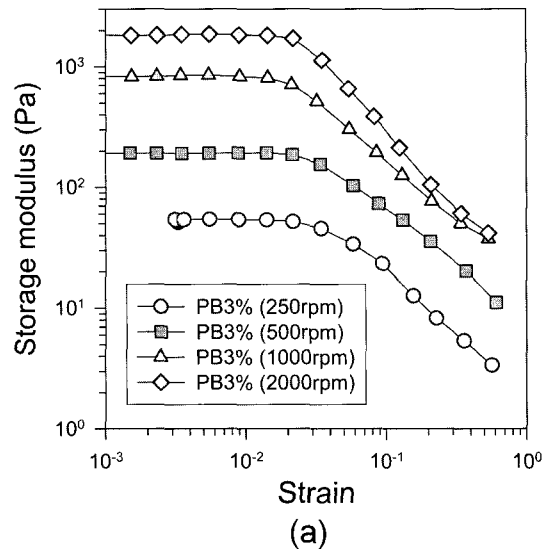


(b)

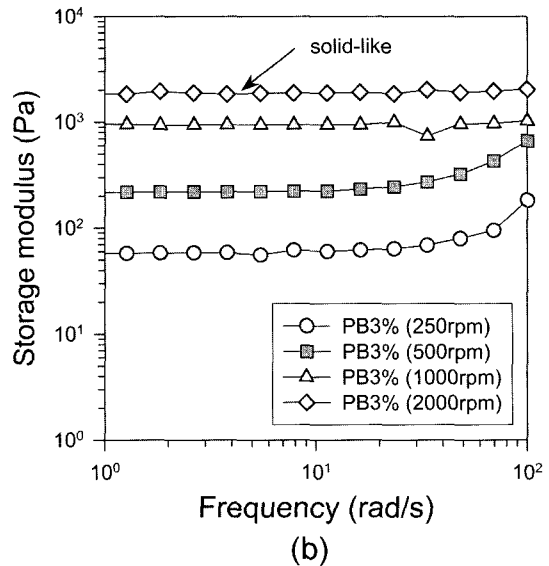
Fig. 4. Creep recovery behavior of HIPES: (a) PB3S500 and (b) PS20S500.

Pa. With the PS20S500 case, the VLE region maintains within the stress of 1 Pa, but fracture or breakdown of emulsion microstructure is already in progress at the stress of 2 Pa. Thus, the yield stress of this emulsion is between 1 and 2 Pa. The yield stress values determined from creep recovery response show good agreement with the values from fluidity measurement aforementioned in Figs. 2 and 3.

The storage modulus data in an oscillatory shear mode are shown in Fig. 5 at different agitation speeds for PB3Sy series. From the strain sweep data shown in Fig. 5(a), the LVE region is maintained up to a strain of 2% at a frequency of 1 rad/s and 0.5% at 100 rad/s (not shown here). Small amplitude oscillatory shear results measured at the



(a)



(b)

Fig. 5. Storage modulus of HIPES depending on agitation speed in an oscillatory mode: (a) strain sweep at a frequency of 1 rad/s and (b) frequency sweep at a strain of 0.5%.

strain of 0.5% are shown in Fig. 5(b). The storage modulus increased with an increase in the agitation speed and the emulsion stability also improved with increasing agitation speed. The reason for these increases in both yield stress and storage modulus is speculated that the radius of the dispersed phase decreased with increasing agitation speed. For the highly concentrated emulsions, the following empirical relations for the yield stress, τ_0 , and the elastic shear modulus, G , were proposed by Princen and Kiss (1989):

$$\tau_0 = \frac{\sigma}{R} \phi^{1/3} (-0.080 - 0.114 \log(1 - \phi)) \quad (1)$$

$$G \cong 1.77 \frac{\sigma}{R} \phi^{1/3} (\phi - \phi_0) \quad (2)$$

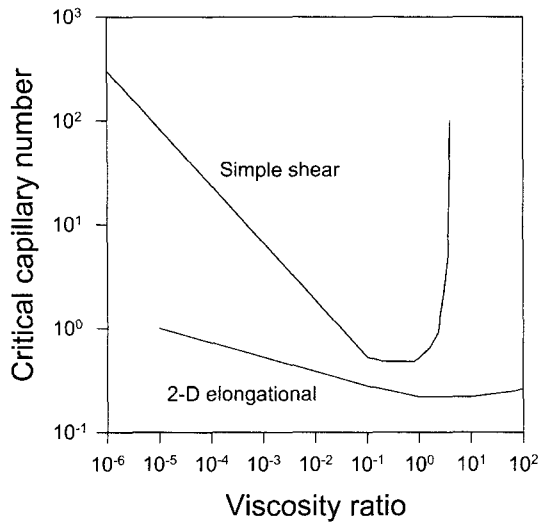


Fig. 6. Critical capillary number for drop breakup as a function of viscosity ratio.

where σ is the interfacial tension, ϕ is the water phase volume and R is the cell radius. Since the emulsions have the same composition, σ and ϕ can be roughly considered to

be constant. Then, it is concluded that the increase in τ_0 and G is ascribed to the decrease in cell size. Quantitative comparison between the equations and the rheological data will require a number of experiments.

The decreasing tendency of cell size when viscosity improvers were added to the oil phase can be explained from a diagram between the critical capillary number and the viscosity ratio as shown in Fig. 6. The critical capillary number is the critical number above which the breakup of drop takes place, and is defined as

$$Ca = \frac{\mu_c \dot{\gamma} R}{\sigma} \quad (3)$$

where μ_c is the viscosity of continuous phase and $\dot{\gamma}$ is the shear rate. The maximum stable drop size can be predicted from the relationship between the critical capillary number and the viscosity ratio. From single-drop experiments, it is known that shear flow does not lead to drop breakup above the viscosity ratio of around 4 (Karam and Bellinger, 1968; Grace, 1982; Janssen and Meijer, 1993). In simple shear flow, the critical capillary number when the viscosity ratio is less than unity increases with the exponent of 0.6 to the viscosity ratio as the viscosity ratio decreases. As a vis-

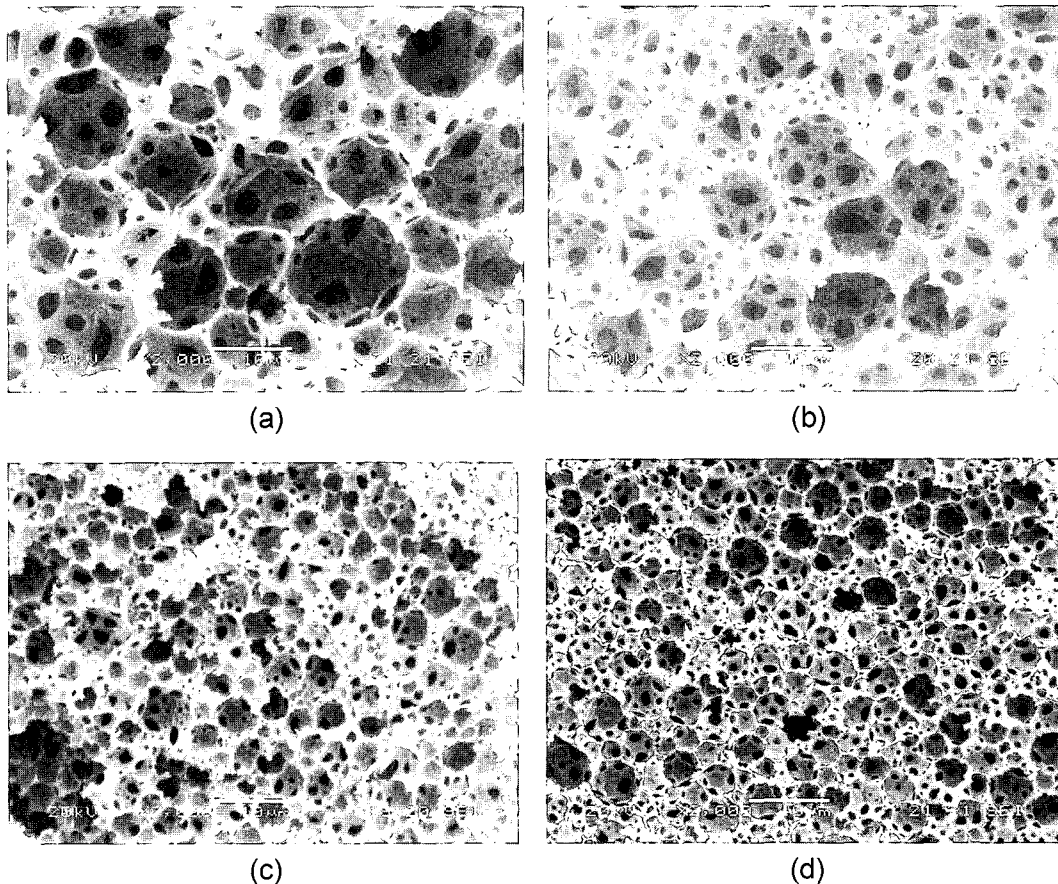


Fig. 7. SEM micrographs of microcellular foams (Scale bars indicate 10 μ m): (a) PB1S500, (b) PB3S500, (c) PB12S500 and (d) PB3S1000.

cosity improver is introduced to the oil phase, the continuous phase viscosity increases and the viscosity ratio decreases. In Equation (3), drop size is inversely proportional to the viscosity of continuous phase at a given capillary number. Thus, the cell size decreases with an exponent of -0.4 as the continuous phase viscosity increases, provided that the dispersed phase viscosity is the same regardless of viscosity improver concentration.

SEM micrographs were taken to examine the microstructural morphology of polyHIPE samples. Fig. 7 shows representative SEM micrographs of microcellular foams for PB_xS_y series. The effect of PB concentration at the agitation speed of 500 rpm can be inferred from Fig. 7(a), (b) and (c). Compared to the sample prepared with lower PB concentration, the sample prepared with higher PB shows smaller cell size. The effect of agitation speed at the PB concentration of 3% can be found from Fig. 7(b) and (d). The sample prepared with higher agitation speed produced much smaller cell size, indicating strong dependency on shear force. Except for the size difference, the morphology of the cell and the open window between adjacent cells seems to be almost identical regardless of agitation speed. Fig. 8 shows representative SEM samples for PS_xS_y series.

Fig. 8(a), (b) and (c) show the effect of PS concentration. Since the solubility of PS in styrene is higher than that of PB, it was possible to dissolve PS in styrene monomer more than 40%, whereas PB could be dissolved up to 12% to keep homogeneous solution. However, the oil phase containing 40% of PS was nearly maximum portion to maintain a stable HIPE in this study. Fig. 8(c) and (d) show the effect of agitation speed at the PS concentration of 20%. The results also show the cell size is strongly dependent upon agitation speed likewise in PB series. Taking both the rheological investigation of HIPEs and the microstructural morphology of polyHIPEs into accounts, there was a qualitative match that average cell size decreased as viscosity improver concentration and agitation speed increased.

Fig. 9 shows the effect of agitation speed on the average cell size of the samples prepared from PB_3S_y series. It clearly shows that the average cell size hyperbolically decreased as the agitation speed increased, since R in Equation (3) is inversely proportional to $\dot{\gamma}$ at a given capillary number when the viscosity ratio is fixed (solid line). The two dashed lines in the figure were plotted based on the hydrodynamic analysis (Shinnar, 1962; Calabrese *et al.*,

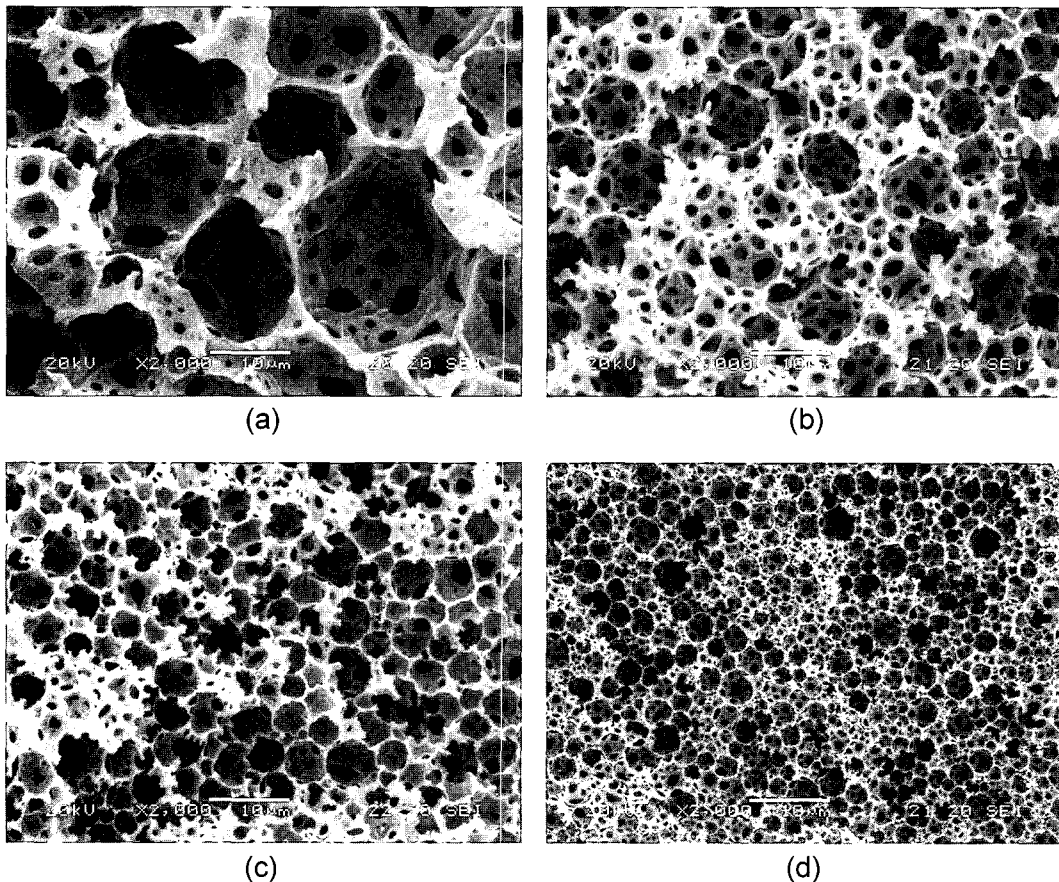


Fig. 8. SEM micrographs of microcellular foams (Scale bars indicate 10 μm): (a) PS5S500, (b) PS12S500, (c) PS20S500 and (d) PS20S1000.

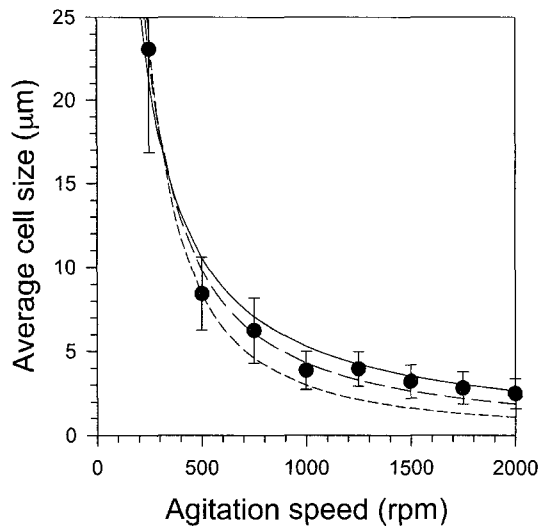


Fig. 9. Effect of agitation speed on the average cell size of the foams (PB3Sy series): solid line is a fit from a power function with the exponent of 1, long-dashed line is a fit with that of 1.2, and short-dashed line is a fit with that of 1.5.

1986; Bourne, 1994; Lee, 1998). A criterion used for the determination of flow ranges is the Kolmogoroff length scale that is defined as

$$\eta = (v_c^3/\varepsilon)^{1/4} \quad (4)$$

where v_c is the kinematic viscosity of continuous phase and ε is the local energy dissipation rate per unit mass. If the maximum stable drop size, d_{max} , is smaller than η , the flow belongs to the viscous shear subrange and the drop breakup would be dominated by viscous force and the drop diameter is proportional to $N^{-1.5}$, where N is the agitation speed. However, if d_{max} is larger than η , then the flow belongs to the inertial subrange and the breakup would be dominated by inertial force and the corresponding exponent on N is -1.2 . Although the hydrodynamic theory was originally developed for highly agitated, dilute dispersion system without any coalescence, a correlation fit was quite satisfactory to HIPE system as well.

4. Conclusions

Open microcellular foams modified by introducing viscosity improvers into conventional water and styrene systems were prepared using the HIPE polymerization technique. Since the foam properties are not separable from the emulsion properties prior to polymerization, the rheological properties of the emulsions were measured to investigate the emulsion stability, the yield stress and the storage modulus. Experimental data were compared with the empirical relations that an increase in the yield stress and the storage modulus is inversely proportional to cell

size, and the results qualitatively followed these relations. Compared to the HIPE foams prepared with conventional formulation, the foams incorporating viscosity improvers showed much finer microcellular morphology. Both the rheological investigation of emulsions and the microstructural morphology of polymerized foams came to a matched conclusion that average cell size decreased as viscosity improver concentration and agitation speed increased. Cell size reduction with viscosity improver concentration could be explained by a dimensional analysis between the capillary number and the viscosity ratio. Hydrodynamic theory developed for highly agitated dispersion was also applied to correlate the average cell size depending on agitation speed, and the correlation fit was quite satisfactory.

Acknowledgement

The author gratefully acknowledges the Korean Science and Engineering Foundation (KOSEF) for the financial support through the Applied Rheology Center, an official engineering research center (ERC) in Korea.

Nomenclature

d_{max}	: maximum stable drop size [m]
Ca	: Capillary number [–]
G	: elastic modulus [Pa]
N	: agitation speed [1/s]
R	: cell radius [m]

Greek letters

$\dot{\gamma}$: shear rate [1/s]
ε	: local energy dissipation rate per unit mass [m ³ /s ²]
ϕ	: volume fraction [–]
η	: Kolmogoroff length scale [m]
μ_c	: continuous phase viscosity [Pa.s]
v_c	: kinematic viscosity of continuous phase [m ² /s]
σ	: interfacial tension coefficient [N/m]
τ_0	: yield stress [Pa]

References

- Barby, D. and Z. Heq, 1982, Low density porous cross-linked polymeric materials and their preparation and use as carriers for included liquids, European Patent 0,060,138.
- Bhumgara, Z., 1995, Polyhipe foam materials as filtration media, *Filtration and Separation* **32**, 245-251.
- Bourne, J.R., 1994, Drop breakup in the viscous subrange: A possible confusion, *Chem. Eng. Sci.* **49**, 1077-1078.
- Calabrese, R.V., T.P.K. Chang and P.T. Dang, 1986, Drop breakup in turbulent stirred-tank contactors. Part I: Effect of dispersed-phase viscosity, *AIChE J.* **32**, 657-666.

- Cameron, N.R. and D.C. Sherrington, 1996, High internal phase emulsions (HIPEs) - structure, properties and use in polymer preparation, *Adv. Polym. Sci.* **126**, 163-214.
- Choi, J.S., B.C. Chun and S.J. Lee, 2003, Effect of rubber on microcellular structures from high internal phase emulsion polymerization, *Macromol. Res.* **11**, 104-109.
- Duke, J.R., M.A. Hoisington, D.A. Langlois and B.C. Benicewicz, 1998, High temperature properties of poly(styrene-co-alkylmaleimide) foams prepared by high internal phase emulsion polymerization, *Polymer* **39**, 4369-4378.
- Grace, H.P., 1982, Dispersion phenomena in high viscosity immiscible fluid systems and application of static mixers as dispersion devices in such systems, *Chem. Eng. Commun.* **14**, 225-277.
- Graessley, W.W., 1984, Viscoelasticity and flow in polymer melts and concentrated solutions, in *Physical Properties of Polymers*, 2nd ed., 134, American Chemical Society, Washington, D. C.
- Janssen, J. M. H. and H. E. H. Meijer, 1993, Droplet breakup mechanisms: Stepwise equilibrium versus transient dispersion, *J. Rheol.* **37**, 597-608.
- Jeoung, H.G., S.J. Ji and S.J. Lee, 2002, Morphology and properties of microcellular foams by high internal phase emulsion polymerization: Effect of emulsion compositions, *Polymer (Korea)* **26**, 759-766.
- Karam, H.J. and J.C. Bellinger, 1968, Deformation and breakup of liquid droplets in a simple shear field, *Ind. Eng. Chem. Fundamentals* **7**, 576-581.
- Lee, S.J., 1998, Prediction of average drop size in turbulently agitated oil-in-oil dispersions, *Korean J. Rheol.* **10**, 1-6.
- Pal, R., 1999, Yield stress and viscoelastic properties of high internal phase ratio emulsions, *Colloid Polym. Sci.* **277**, 583-588.
- Park, C.I., W.G. Cho and S.J. Lee, 2003, Emulsion stability of cosmetic creams based on water-in-oil high internal phase emulsions, *Korea-Australia Rheol. J.* **15**, 125-130.
- Princen, H.M., 1983, Rheology of foams and highly concentrated emulsions: I. Elastic properties and yield stress of a cylindrical model system, *J. Colloid Interface Sci.* **91**, 160-175.
- Princen, H.M. and A.D. Kiss, 1989, Rheology of foams and highly concentrated emulsions: IV. An experimental study of the shear viscosity and yield stress of concentrated emulsions, *J. Colloid Interface Sci.* **128**, 176-187.
- Shinnar, R., 1961, On the behavior of liquid dispersions in mixing vessels, *J. Fluid Mech.* **10**, 259-275.
- Stokes, R.J. and D.F. Evans, 1997, *Fundamentals of Interfacial Engineering*, 263-268, Wiley-VCH, New York.
- Wakeman, R.J., Z.G. Bhungara and G. Akay, 1998, Ion exchange modules formed from polyhipe foam precursors, *Chem. Eng. J.* **70**, 133-141.
- Williams, J.M. and D.A. Wroblewski, 1988, Spatial distribution of the phases in water-in-oil emulsions. Open and closed microcellular foams from cross-linked polystyrene, *Langmuir* **4**, 656-662.